Journal of Thermal Analysis and Calorimetry, Vol. 94 (2008) 2, 567–577

SOME NOVEL TETRADENTATE SCHIFF BASE COMPLEXES VO(IV) AND Cu(II) INVOLVING FLUORINATED HETEROCYCLIC β-DIKETONES AND POLYMETHYLENE DIAMINES OF VARYING CHAIN LENGTH
Synthesis, spectral, coordination and thermal aspects

C. K. Modi[1*] *and B. T. Thaker*[2]

[1]Department of Chemistry, Sardar Patel University, Vallabh Vidyanagar, 388 120, Gujarat, India
[2]Department of Chemistry, Veer Narmad South Gujarat University, Surat, 395 007, Gujarat, India

The present article describes the synthesis, spectral, coordination and thermal aspects of N,N'-polymethylene *bis*(1-phenyl-3-methyl-4-trifluoroacetylimino-2-pyrazoline-5-ol)oxovanadium(IV) or copper(II) Schiff base complexes with alkyl backbones ranging from two to four carbons have been characterized on the basis of elemental analysis, magnetic moments, molar conductivity measurements, spectra (FTIR, ESR, UV-Visible, MS), VPO and thermal studies. The vapour pressure osmometry (VPO) and mass spectral studies indicate that the complexes are monomeric. An ESR study of all these complexes of VO(IV) and Cu(II) are consistent with the square pyramidal and square planar geometries of these metal ions, respectively. In addition, the kinetics and thermodynamic parameters for the different thermal decomposition steps of the complexes have been studied employing Horowitz–Metzger and Freemen–Carroll methods.

Keywords: *mononuclear VO(IV) and Cu(II) complexes, novel tetradentate Schiff bases (H_2TSB-n), spectroscopic, TG/DTG and DSC studies, VPO*

Introduction

Transition metal complexes of tetradentate Schiff base ligands find applications as models of certain metal enzymes and in catalysis and materials chemistry [1]. A series of tetradentate Schiff base complexes of the type M(Sal-*n*) [where M=oxovanadium(IV) and copper(II)] with *n*=2–10 have been studied extensively [2–5].

Thermogravimetry is a process in which a substance is decomposed in the presence of heat, which causes bonds the molecules to be broken [6, 7]. The thermal analysis techniques were widely applied in studying of thermal behaviour of metal complexes [8–11]. The thermal behaviors of mixed-ligand complexes involving pyrazolone derivatives were studied by Xu *et al.* [12]. In continuation of our earlier work [13–16] herein we describe synthetic, thermal, spectroscopic and coordination aspects of some novel tetradentate Schiff base complexes of VO(IV) and Cu(II) involving fluorinated heterocyclic β-diketones and polymethylene diamines. The suggested structure of the Schiff bases (H_2TSB-*n*) is shown in Scheme 1.

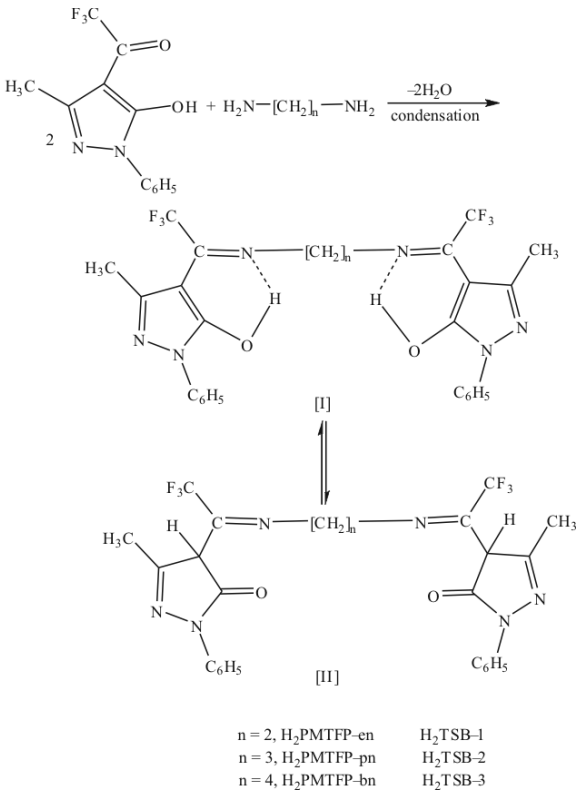

n = 2, H_2PMTFP–en H_2TSB–1
n = 3, H_2PMTFP–pn H_2TSB–2
n = 4, H_2PMTFP–bn H_2TSB–3

Scheme 1 Suggested structure of the Schiff bases (H_2TSB-*n*)

* Author for correspondence: chetank.modi1@gmail.com

1388–6150/$20.00

Akadémiai Kiadó, Budapest, Hungary
Springer, Dordrecht, The Netherlands

Experimental

Materials

Reagent and solvents

All the chemicals used were of analytical grade and used without further purification. The organic solvents were purified by standard methods [17].

Synthesis of tetradentate Schiff base ligands (H_2TSB-*n*)

The Schiff base ligands (H_2TSB-*n*) used in the present investigation is the condensation products of HPMTFP and alkyl diamines [ethylene diamine (en), propylene diamine (pn) or butylene diamine (bn)] in 2:1 molar ratio. The reaction leading to the formation of the Schiff bases as discussed below.

Synthesis of 1-phenyl-3-methyl-4-trifluoroacetyl-2-pyrazoline-5-one (HPMTFP)

The ligand HPMTFP was synthesized by using a procedure that reported by Okafor earlier [18]. Yield: 74%, *m.p*. 144°C. Anal. calc. for $C_{12}H_9N_2O_2F_3$: C, 53.34; H, 3.35; N, 10.49. Found: C, 53.27; H, 3.36; N, 10.49%. ^{1}H NMR (300 MHz, $CDCl_3$): δ (ppm)=2.47 (s, 3H, $–CH_3$); 7.28–7.86 (m, 5H, Ph); 12.20 (s, 1H, –OH).

Synthesis of N,N'–ethylene *bis*(1-phenyl-3-methyl-4-trifluoroacetylimino-2-pyrazoline-5-ol) (H_2TSB-1)

An ethanolic solution (50 mL) of 1-phenyl-3-methyl-4-trifluoroacetyl-2-pyrazoline-5-one (2.70 g, 10 mmol) and an ethanolic solution (25 mL) of ethylene diamine (5 mmol, 0.33 mL) in 2:1 molar ratio were mixed with constant stirring. Refluxing was carried out for 2 h. The solution was cooled overnight at room temperature. The formed pinkish brown crystals were collected and dried in air, yield 80%, *m.p*. 90°C. Anal. calc. for $C_{26}H_{22}N_6O_2F_6$: C, 55.30; H, 3.90; N, 14.89. Found: C, 55.30; H, 3.88; N, 14.82%. FTIR (cm^{-1}), ν_{max} (KBr): 3354b (OH–N), 1623s ($C{=}N_{azomethine}$), 1588w ($C{=}N_{cyclic}$), 1350s (C–O). ^{1}H NMR (300 MHz, DMSO-d_6): δ (ppm)=2.21 (s, 3H, $–CH_3$); 3.40–3.47 (m, 4H, $–CH_2–$ bridge); 7.17–7.96 (m, 5H, Ph); 9.25 (s, 1H, OH…N).

Synthesis of N,N'–propylene *bis*(1-phenyl-3-methyl-4-trifluoroacetylimino-2-pyrazoline-5-ol) (H_2TSB-2)

The Schiff base (H_2TSB-2) was prepared the same way as H_2TSB-1 was prepared. Yield 72%, *m.p*. 92°C. Anal. calc. for $C_{27}H_{24}N_6O_2F_6$: C, 56.15; H, 4.13; N, 14.53. Found: C, 56.10; H, 4.10; N, 14.49%. FTIR (cm^{-1}), ν_{max} (KBr): 3384b (OH–N), 1620s ($C{=}N_{azomethine}$), 1590w ($C{=}N_{cyclic}$), 1352s (C–O). ^{1}H NMR (300 MHz, DMSO-d_6): δ (ppm)=2.19 (s, 3H, $–CH_3$); 1.21–2.16 (m, 6H, $–CH_2–$ bridge); 7.17–7.82 (m, 5H, Ph); 9.26 (s, 1H, OH…N).

Synthesis of N,N'–butylene *bis*(1-phenyl-3-methyl-4-trifluoroacetylimino-2-pyrazoline-5-ol) (H_2TSB-3)

The Schiff base H_2TSB-3 was prepared the same way as H_2TSB-1 was prepared. Yield 70%, *m.p*. 99°C. Anal. calc. for $C_{28}H_{26}N_6O_2F_6$: C, 56.75; H, 4.39; N, 14.18. Found: C, 56.71; H, 4.32; N, 14.12%. FTIR (cm^{-1}), ν_{max} (KBr): 3340b (OH–N), 1622s ($C{=}N_{azomethine}$), 1585w ($C{=}N_{cyclic}$), 1355s (C–O). ^{1}H NMR (300 MHz, DMSO-d_6): δ (ppm)=2.18 (s, 3H, $–CH_3$); 1.44–2.00 (m, 8H, $–CH_2–$ bridge); 7.07–7.85 (m, 5H, Ph); 9.42 (s, 1H, OH…N).

Synthesis of metal complexes

The solution of $VOSO_4{\cdot}5H_2O$ (1.45 g, 5 mmol) or $CuSO_4{\cdot}5H_2O$ (1.25 g, 5 mmol) in 25 mL of hot methanol was added to a 25 mL of methanolic solution of the various Schiff bases (H_2TSB-*n*) [H_2TSB-1 (2.82 g, 5 mmol), H_2TSB-2 (2.89 g, 5 mmol) and H_2TSB-3 (2.96 g, 5 mmol)] in 1:1 molar ratio. The pH of the solution was adjusted 5–6 by drop wise addition of methanolic solution of sodium acetate in it. The resulting mixture was heated under reflux on a water bath for 2–3 h. The obtained coloured precipitate was filtered off, washed with hot water, hot methanol and diethyl ether and finally dried in a vacuum desiccator over anhydrous $CaCl_2$.

Physical measurements

Elemental analyses (C, H, N) were performed at CDRI, Lucknow with a Carlo Ebra 1108 analyzer. The copper content of the complexes were analyzed by the EDTA titration technique [19]. Infrared spectra were recorded with a Perkin-Elmer IR spectrophotometer (4000–400 cm^{-1}) using KBr pellets. ^{1}H NMR and ESR spectra were recorded at RSIC, IIT, Powai, Mumbai. The number average molecular mass (*Mn*) of the complexes were measured by a VPO (Knaur, Germany) using DMF as a solvent and polystyrene (PS) as a calibrant. The electronic spectra were recorded on Shimadzu 160A UV-visible spectrophotometer using DMSO as the solvent blank. The magnetic moments were obtained by the Gouy's method using mercury tetrathiocyanato cobaltate(II) as a calibrant (χ_g=16.44·10^{-6} c.g.s. units at 20°C). The FAB mass spectra were recorded on a JEOL SX 102/DA-6000 Mass Spectrometer. A simul-

taneous TG/DTG have been obtained by a model Pyris-1 TGA, Perkin Elmer, USA. The DSC was recorded using DSC 2920, TA Instrument, USA.

Results and discussion

The analytical and physical data of the complexes are presented in Table 1. The complexes are colored and stable in air. They are insoluble in water and in most organic solvents but soluble in DMF. The molar conductances of 10^{-3} M DMSO solutions of the compounds lie in the range 0.02–0.05 Ω^{-1} cm^2 mol^{-1}showing that the complexes are non-electrolytes. The formations of the complexes are assumed according to the balanced chemical Eq. (1).

$$VOSO_4{\cdot}5H_2O+H_2TSB\text{-}n\rightarrow [VO(TSB\text{-}n)]{\cdot}0.5H_2O+H_2SO_4+4.5H_2O$$

$$CuSO_4{\cdot}5H_2O+H_2TSB\text{-}n\rightarrow [Cu(TSB\text{-}n)]{\cdot}1.5H_2O+H_2SO_4+3.5H_2O$$

Infrared spectra

In order to study the binding mode of Schiff base to the metal ion in the complexes, the IR spectra of Schiff bases (H_2TSB-*n*) were compared with the spectra of the corresponding complexes. In the investigated Schiff bases, a broad band observed between 3340–3384 cm^{-1} is attributed to $\nu_{(OH)}$. However free $\nu_{(OH)}$ is generally observed at or above 3450 cm^{-1}; the observed lower value is due to intramolecular H-bonding and therefore structure [I] in Scheme 1 is favoured. The $\nu_{(C-O)}$ band is raised by 10–15 cm^{-1} in the spectra of complexes to the position observed in the Schiff bases (H_2TSB-*n*) suggesting the coordination via this oxygen [20]. The strong band at ~1620 cm^{-1} attributable to the C=N stretching vibration of the Schiff base ligands is shifted to a region of 1600–1605 cm^{-1} in the complexes, indicating the coordination of the azomethine nitrogen [21]. The oxovanadium(IV) complexes exhibit an additional strong absorption band near ~958 cm^{-1}, which has been assigned to $\nu_{(V=O)}$ [22]. In the far–IR region, two new bands at 515–550 and 412–482 cm^{-1} in the complexes are assigned to $\nu_{(M-N)}$ [23] and $\nu_{(M-O)pyrazolone}$ groups, respectively. All of these data confirm the fact that H_2TSB-*n* behaves as a dinegative tetradentate ligand forming a conjugated chelate ring, with the ligand exists in the complexes in the enolized form.

Vapour pressure osmometry (VPO)

The number average molecular mass ($\overline{Mn}$) of some complexes was estimated by vapour pressure osmometry [24]. The plot of millivolts *vs.* concentration was drawn. With the help of the slope and the VPO constant *K*, the $\overline{Mn}$ value of the complexes were calculated (Table 1).

Mass spectral studies

The recorded mass spectra and the molecular ion peak for the complex [VO(TSB-1)]·0.5H_2O have been used to confirm the molecular formulae. Calculated and found molecular masses are given in Table 1. The mass spectrum of [VO(TSB-1)]·0.5H_2O shows multipeaks corresponding to the successive degradation of the molecule as shown in Fig. 1 and its fragmentation pattern is given in Scheme 2. The first peak at *m/e* 629 represents the molecular ion peak of the complex with 9.72% abundance. The sharp peak (base peak) ob-

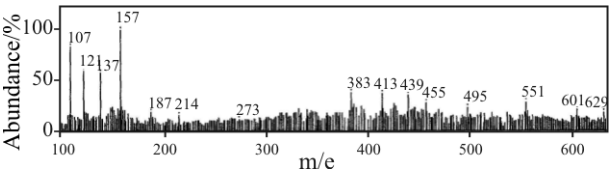

Fig. 1 The mass spectrum of [VO(TSB-1)]·0.5H_2O

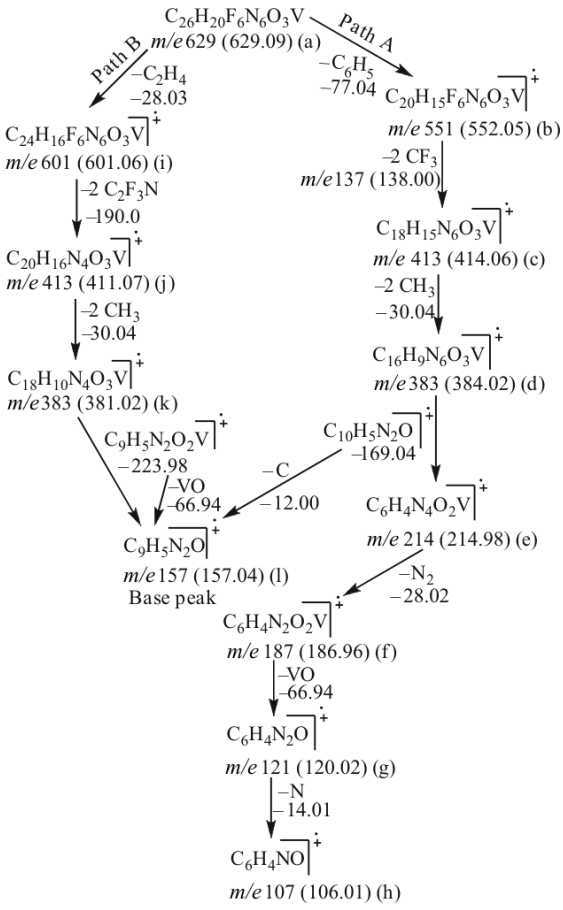

Scheme 2 Suggested fragmentation pattern of [VO(TSB-1)]·0.5H_2O

Table 1 Physical, analytical data and formula masses (F. W.) of the complexes

Complex	Colour/ yield/ %	$\overline{Mn}$/ g mol^{-1}	Elemental analysis/% found/required				Λ/Ω^{-1} cm^2 mol^{-1}	μ_{eff}/B.M.	F.W.	
			C	H	N	M			found*	calcd
[VO(TSB-1)]·0.5H_2O	Dark green/ 76	636.77	48.98/48.94	3.31/3.32	13.20/13.17	8.08/7.98	0.027	1.68	629.0	629.09
[VO(TSB-2)]·0.5H_2O	Dark green/ 78	654.15	49.74/49.72	3.58/3.55	12.94/12.89	7.83/7.81	0.020	1.74	–	643.11
[VO(TSB-3)]·0.5H_2O	Dark green/ 76	–	50.53/50.48	3.77/3.78	12.59/12.62	7.69/7.65	0.021	1.79	–	657.13
[Cu(TSB-1)]·1.5H_2O	Green/ 79	653.78	47.88/47.89	3.53/3.55	12.92/12.89	9.83/9.74	0.042	1.72	624.0	625.08
[Cu(TSB-2)]·1.5H_2O	Green/ 78	–	48.65/48.68	3.79/3.78	12.64/12.62	9.57/9.54	0.048	1.76	640.0	639.10
[Cu(TSB-3)]·1.5H_2O	Green/ 76	681.68	49.49/49.45	4.06/4.00	12.41/12.36	9.39/9.34	0.051	1.78	654.0	653.12

*values obtained from mass spectra

served at *m/e* 157 represents the stable species $[C_9H_5N_2O]^+$ ion with 99.41% abundance.

Magnetic properties and electronic spectra

The $[VO(TSB)]\cdot 0.5H_2O$ complexes exhibit μ_{eff} value (Table 1) between 1.68–1.79 B.M., which are very close to spin only value for d^1 case [25]. This indicates that the compounds are monomeric and there may not be intermolecular association in solid state. The electronic spectra of the VO(IV) complexes show one prominent maxima between 22421–22988 cm^{-1} and a red shoulder at 17544–18518 cm^{-1}. The third band is very weak and observed at 10471–11737 cm^{-1}. In principle, oxovanadium compound could either be mononuclear with V=O or could be polynuclear with –V–O–V–O bridge bond. In the present complexes, evidences FAB-mass and VPO studies suggest that the compounds are mononuclear. Thus keeping in view, the tetradentate nature of the Schiff bases, 5-coordinated square-pyramidal structures with C_{4V} symmetry, in which the Schiff base lies in the basal plane and O at the apical position may be suggested for all the complexes.

The magnetic moment of $[Cu(TSB)]\cdot 1.5H_2O$ complexes are observed in the range of 1.72–1.78 B.M., which corresponds to a single unpaired electron with a very slight orbital contribution. The electronic spectra of $[Cu(TSB)]\cdot 1.5H_2O$ complexes show well resolved band observed at 12270, 13263 and 12063 cm^{-1} in $[Cu(TSB\text{-}1)]\cdot 1.5H_2O$, $[Cu(TSB–1)]\cdot 1.5H_2O$ and $[Cu(TSB\text{-}1)]\cdot 1.5H_2O$ complexes, respectively. On the other hand, the broad shoulder observed at 16393, 16129 and 16000 cm^{-1}. These *d–d* transitions are shifted to lower energy as the methylene (CH_2) numbers increases. Absence of any band below 10000 cm^{-1}, ruled out the possibility of tetrahedral structure for the complexes. Thus, square-planar geometry is proposed for all the complexes in the present study.

ESR spectral studies

$[VO(TSB)]\cdot 0.5H_2O$ and $[Cu(TSB)]\cdot 1.5H_2O$

ESR spectra for $[VO(TSB)]\cdot 0.5H_2O$ and $[Cu(TSB)]\cdot 1.5H_2O$ complexes have been recorded for polycrystalline and solution (50:50, DMSO:$CHCl_3$) at RT and LNT. Spectra of polycrystalline samples give one signal in oxovanadium(IV) compounds. The *g* values ~1.99 are invariably lower than the free electron value (g_e=2.0023). This lowering is related to the spin-orbit interaction of the ground state, d_{xy} level. The spectra of DMSO:$CHCl_3$ (50:50) mixed solvents yielded isotropic asymmetrical eight lines at RT except $[VO(TSB\text{-}3)]\cdot 0.5H_2O$. In the frozen solutions, the anisotropic spectra of the complexes exhibit axial rather than rhombic symmetry. The Hamiltonian parameters $g_\parallel$, $g_\perp$, $|g|$, $A_\parallel$ and $A_\perp$ were calculated and are included in Table 3. The values are in accordance with that of a molecule which exists in square pyramidal geometry [26–28]. The molecular orbital coefficients α^2 (covalent in-plane σ-bonding) and β^2 (covalent in-plane π-bonding) were calculated by using the reported equations [29] (Table 2). This suggests the equal amount of covalency between M–L bonding in the present complexes. The γ, the bonding coefficient for d_{xy} and d_{yz} orbitals, measures the covalency of the V=O bonds.

For Cu(II) complex, the *g* values indicate that $g_\parallel > g_\perp > 2.0023$ in all the cases. Further, $|g|$ values 2.08–2.13 are indicative of square planar geometry for Cu(II) complexes. *G* values measure the exchange interaction between copper centers in polycrystalline state. In the present complexes $G>4$ suggests that the exchange interaction is negligible and the ligand strength is moderate [30]. The ESR spectra of Cu(II) complexes in solution state at RT are isotropic probably due to tumbling motions of the molecules. The isotropic value $|g|$ is calculated at the center of the four lines spectrum. The isotropic nuclear hyperfine constant $|A|$ is calculated from the separation between two adjacent lines of the spectrum. However, these compounds, in solution at 77 K (frozen state) show three well resolved, moderate intensity peaks, in the parallel part and eight lines in the perpendicular part, is due to super hyperfine splitting of nearby nitrogen of Schiff base ligand. Hamiltonian parameters $g_\parallel$, $g_\perp$, $|g|$, $A_\parallel$ and $A_\perp$ were calculated and are summarized in Table 2. For Cu(II) complex, $g_\parallel$ is a parameter sensitive enough to indicative covalence. Generally $g_\parallel$ value for covalent complexes is $g_\parallel < 2.3$, and for ionic $g_\parallel \geq 2.3$. The $g_\parallel$ values (Table 2) for all the complexes are almost same, i.e. 2.27, which indicates that the covalent nature of M–L bond in these complexes. The ratio of $g_\parallel/A_\parallel$ is used to find the structure of a complex. In the present Cu(II) complexes, the ratio obtained is in the range 126.57–130.92 cm, which falls in the range 90–140 cm for square-planar copper(II) complexes [31].

Molecular orbital co-efficient, α^2 (covalent in-plane σ-bonding) and β^2 (covalent in-plane π-bonding) (Table 2) were calculated [32]. For present $[Cu(TSB)]\cdot 1.5H_2O$ complexes, the values of α^2 are in the range of 0.79–0.81, indicating moderate covalency for σ-bonding. The in-plane π-bonding parameter β^2 has more potential interest that α^2 as it should be sensitive to the back donation from d_{xy} orbital of the Cu to the π^* anti-bonding orbital of the ligand. The calculated values of β^2 are found between 0.59–0.66. This suggests that the back donation in the present complexes is significant.

Table 2 *g* and *A* values of solution[a] ESR spectra and bonding parameters of VO(IV) and Cu(II) complexes

Complexes	$g_{\parallel}$	$g_{\perp}$	$\lvert g\rvert$	$A_{\parallel}\cdot10^{-4}/cm^{-1}$	$A_{\perp}\cdot10^{-4}/cm^{-1}$	$\lvert A\rvert$	$g_{\parallel}/A_{\parallel}$	α^2	β^2	γ^2	α^2_{Cu}
$[VO(TSB\text{-}1)]\cdot0.5H_2O$	1.94	1.99	1.97	162.38	41.74	81.94	–	1.10[c] (1.17)[d]	0.74 (0.69)[d]	0.56 (0.59)[d]	–
$[VO(TSB\text{-}2)]\cdot0.5H_2O$	1.93	1.99	1.97	170.04	46.43	87.96	–	1.14 (1.21)[d]	0.75 (0.71)[d]	0.39 (0.40)[d]	–
$[VO(TSB\text{-}3)]\cdot0.5H_2O$	–	–	–	–	–	–	–	–	–	–	–
$[Cu(TSB\text{-}1)]\cdot1.5H_2O$	2.26	2.02	2.11	170.38 (14.06)[b]	31.22 (10.50)[b]	78.61 (12.87)[b]	130.92	0.79[e]	0.62	–	0.75
$[Cu(TSB\text{-}2)]\cdot1.5H_2O$	2.27	2.01	2.10	179.34 (14.00)[b]	42.46 (10.50)[b]	88.09 (12.82)[b]	126.57	0.81	0.66	–	0.81
$[Cu(TSB\text{-}3)]\cdot1.5H_2O$	2.27	2.02	2.10	178.64 (14.02)[b]	42.78 (10.51)[b]	88.01 (12.85)[b]	127.52	0.81	0.59	–	0.81

[a](50% DMSO+50% $CHCl_3$): [b]corresponding nitrogen super hyperfine splitting constant, [c]values calculated using P=128; [d]values calculated using P=136 and [e]values calculated using P=0.036

Table 3 Thermoanalytical results (TG, DTG and DSC) of VO(IV) and Cu(II) complexes

Complex	TG range/°C	DTG_{max}/°C	DSC_{max}/°C	Mass loss/% obs. (calc.)	Assignment
$[VO(TSB\text{-}1)]\cdot0.5H_2O$	40–150	–	–	1.44 (1.41)	Loss of half mole of lattice water molecule
	150–300	280	261(–)	50.37	Removal of one part of the ligand
	300–810	336	301(–)	39.91	Removal of remaining part of the ligand
				91.72* (92.02)	Leaving free metal residue
$[VO(TSB\text{-}2)]\cdot0.5H_2O$	40–140	–	–	1.53 (1.38)	Loss of half mole of lattice water molecule
	140–290	272	259(+)	48.92	Removal of one part of the ligand
	290–780	316	297(–)	37.02	Removal of remaining part of the ligand
				87.47* (87.25)	Leaving VO_2 residue
$[VO(TSB\text{-}3)]\cdot0.5H_2O$	40–140	–	–	1.48 (1.35)	Loss of half mole of lattice water molecule
	140–310	261	264(+)	49.37	Removal of one part of the ligand
	310–780	310	–	36.17	Removal of remaining part of the ligand
				87.02* (87.52)	Leaving VO_2 residue
$[Cu(TSB\text{-}1)]\cdot1.5H_2O$	40–150	–	115(+)	4.06 (4.14)	Loss of 1.5 moles of lattice water molecules
	150–530	256	239(–)	47.45	Removal of one part of the ligand
	530–760	689	–	36.26	Removal of remaining part of the ligand
				87.77* (87.86)	Leaving CuO residue
$[Cu(TSB\text{-}2)]\cdot1.5H_2O$	40–130	94	116(+)	4.14 (4.05)	Loss of 1.5 moles of lattice water molecules
	130–510	242	227(–)	48.32	Removal of one part of the ligand
	510–740	646	–	35.62	Removal of remaining part of the ligand
				88.08* (88.06)	Leaving CuO residue
$[Cu(TSB\text{-}3)]\cdot1.5H_2O$	40–140	89	107(+)	4.08 (3.97)	Loss of 1.5 moles of lattice water molecules
	140–490	239	221(–)	49.54	Removal of one part of the ligand
	490–710	–	–	34.66	Removal of remaining part of the ligand
				88.28* (88.31)	Leaving CuO residue

(+): endothermic; (–): exothermic; * Total mass loss

Thermal studies

Each step of decomposition in most of the thermal reactions of the solids follows the trend

$$\text{solid-1} \xrightarrow{\text{heat}} \text{solid-2+gas} \quad (1)$$

This process comprises of several stages such as the chemical act of breaking of bonds, breakdown of the solid-1 crystal lattice, formation of the crystal lattice of the solid-2, absorption–desorption of the gaseous products, diffusion of gas and heat transfer etc. The rate of the thermal decomposition is determined by the rate of one or more of these stages and sometimes, the rate determining step changes during the process.

The first order reaction may be described by the equation,

$$d\alpha/dt=k(1-\alpha)^n \quad (2)$$

where α is the volume fraction reacted at time t and n is the order of reaction. The constant k is related to the absolute temperature by an Arrhenius type equation,

$$k=A\exp(-E_a/RT) \quad (3)$$

where A is constant and E_a is the energy of activation.

For the determination of various kinetic parameters, numerous methods have been described in the literature. However, in the present communication, the methods reported by Freeman–Carroll [33] and Horowitz and Metzger [34] have been adopted. The later method is based on two assumptions: (a) thermal and diffusion barriers are negligible and (b) the Arrhenius equation is valid (Eq. (3) above). Horowitz and Metzger have derived the relation:

$$\log[1-(1-\alpha)^{1-n}/(1-n)]=E_a\theta/2.303RTs^2 \text{ for } n\neq 1 \quad (4)$$

For the first order relation, i.e. n=1, the left hand side of Eq. (4) would be log[–ln/1–α]. Therefore, for the first order kinetic process the Horowitz–Metzger equation may be written in the form:

$$\log[\log w_\infty/w_r]=E_a\theta/2.303RT_s^2-\log 2.303 \quad (5)$$

where $w_r=w_\infty - w$; w_∞ is the mass loss at the completion of the reaction; w is the mass loss up to time t; $\theta=T-T_s$, T is the absolute temperature at time t and T_s is the peak temperature which is directly taken from the DTG curve, R is a gas constant and E_a is the energy of activation. The plots of log[log$w\infty/w_r$] *vs.* θ were drawn and the energy of activation E_a was calculated from the slopes of these plots for a particular stage. The typical Horowitz–Metzger plot for the thermal degradation of [VO(TSB-1)]·0.5H_2O is shown in Fig. 2.

In the differential method of Freeman–Carroll, the equation was used in the following form:

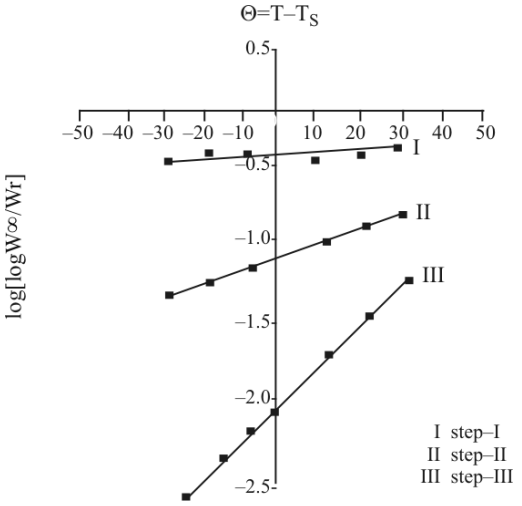

Fig. 2 Horowitz–Metzger plot for the thermal degradation of [VO(TSB-1)]·0.5H_2O

$$[(-E_a/2.303R)\Delta(1/T)]/\Delta\log w_r= -n+\Delta\log(dw/dt)/\Delta\log w_r \quad (6)$$

where T is the temperature in K, R is gas constant, $w_r=w_c-w$; w_c is the mass loss at the completion of the reaction and w is the total mass loss up to time t. E_a and n are the energy of activation and order of reaction, respectively. A typical curve of [Δlog(dw/dt)/$\Delta\log w_r$] *vs.* [$\Delta(1/T)/\Delta\log w_r$] for the [VO(TSB-1)]·0.5H_2O complex is shown in Fig. 3. The slope of the plot gave the value of $E_a/2.303R$ and the order of reaction (n) was determined from the intercept.

The thermal behavior of the prepared complexes

The thermal behaviour of the synthesized complexes has been characterized on the basis of TG/DTG and DSC methods. TG curve of [VO(TSB-1)]·0.5H_2O and [Cu(TSB-1)]·1.5H_2O are taken as representative examples for the decomposition of these complexes. Thermoanalytical data of the complexes are given in Table 3.

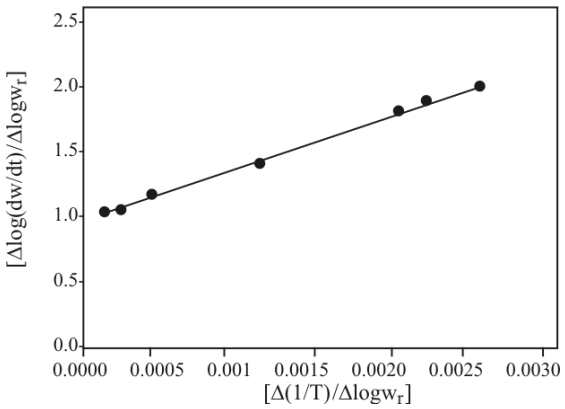

Fig. 3 Freeman–Carroll plot for the thermal degradation of [VO(TSB-1)]·0.5H_2O

[VO(TSB-1)]·0.5H_2O

TG/DTG and DSC curves of the complex [VO(TSB-1)]·0.5H_2O represented in Figs 4 and 5, respectively. The decomposition of the complex undergoes in three stages. The first mass loss (obs. 1.44%; calcd. 1.41%) in the temperature range 40–150°C, corresponds to the loss of half mole of lattice water molecule. The loss of half mole of lattice water molecule is of zero order reaction and the value of the energy of activation for the dehydration process is found to be 3.21 kJ mol^{-1}. With heating; the decomposition of the ligand moiety was followed. Two well-separated peaks are displayed on the DTG curve; this indicates that the decomposition of the ligand divides into two steps. The second stage, which occurs in the temperature range 150–300°C, with a DTG peak at 280°C, corresponds to the decomposition of one part of the ligand. The observed mass loss for this stage is 50.37%. It is further supported by an exothermic peak at 261°C in DSC curve. The third stage occurs between 300 and 810°C, corresponding to the decomposition of the remaining part of the ligand, with the mass loss of 39.91%. The maximum rate of mass loss is indicated by the DTG peak at 336°C. The total mass loss (91.72%) coincides with the theoretical value of 92.02% (Table 3). The final residue, estimated as free vanadium [35] atom, has the observed mass 8.27% as *vs.* the calculated value of 7.98%.

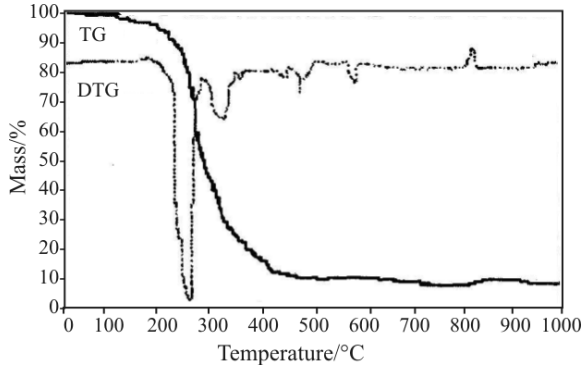

Fig. 4 TG/DTG curves of [VO(TSB-1)]·0.5H_2O

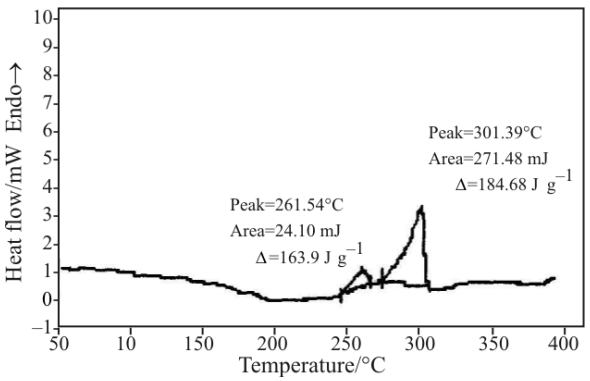

Fig. 5 DSC curve of [VO(TSB-1)]·0.5H_2O

[Cu(TSB-1)]·1.5H_2O

The thermal decomposition of the complex [Cu(TSB-1)]·1.5H_2O undergoes in three stages. The first endothermic peak [36] in DSC at 115°C, in the temperature range 40–150°C, with the mass loss (obs. 4.06%; calcd. 4.14%) corresponds to the loss of one and half moles of lattice water molecules. The loss of one and half moles of lattice water molecules is of zero order reaction and the value of the energy of activation for the dehydration process is found to be 4.86 kJ mol^{-1}. The second stage, which occurs in the temperature range 150–530°C with a DTG peak at 256°C, is corresponding to the decomposition of one part of the ligand. The observed mass loss for this stage is 47.45%. This process is further supported by an exothermic peak at 239°C in DSC curve. The third stage is related to the decomposition of the remaining part of the ligand in the temperature range of 530–760°C with a DTG peak at 689°C, accompanied by a mass loss of 36.26%. The overall mass losses are observed to be 87.77%, which is in well agreement with the calculated value of 87.86%. The final residue, estimated as copper oxide, has the observed mass 12.12% as against the calculated value of 12.01%.

Non-isothermal calculations were used extensively to evaluate kinetic parameters such as activation entropy ($\Delta S^{\#}$), activation enthalpy ($\Delta H^{\#}$) and the free energy of activation ($\Delta G^{\#}$) for the different thermal decomposition steps in the complexes employing the Horowitz–Metzger equations [34] are given in Table 4. The kinetic parameters calculated by the Horowitz–Metzger method revealed no significant difference with that evaluated by the Freeman–Carroll method. The negative $\Delta S^{\#}$ values for all decomposition steps in the complexes indicate that the complexes are more ordered [37]. The complexes decomposed in mainly three-step processes and it was observed that the first dehydration step in all complexes are of zero order reactions whereas, the remaining decomposition steps are of first order reactions. The activation energy values of third step, the high value of E_a for all the complexes, indicate that the removed part is strongly bonded to the metal ion. The kinetic parameters, especially activation energy (E_a) is helpful in assigning the strength of the bonding of ligand moieties with the metal ion. The relative high E_a values of Cu(II) complexes than VO(IV) complexes (Table 4) indicates that the ligand is strongly bonded to the metal ion [38]. Based on the activation energy values, VO(IV) complexes show a lower thermal stability than Cu(II) complexes. This can be discussed in terms of repulsion among electron pairs in

Table 4 Thermodynamic data of the thermal decomposition of VO(IV) and Cu(II) complexes

Complex	TG range/°C	Freeman–Carroll method					Horowitz–Metzger method			
		E_a/ kJ mol^{-1}	n	$\Delta S^{\#}$/ J K^{-1} mol^{-1}	$\Delta H^{\#}$/ kJ mol^{-1}	$\Delta G^{\#}$/ kJ mol^{-1}	E_a/ kJ mol^{-1}	$\Delta S^{\#}$/ J K^{-1} mol^{-1}	$\Delta H^{\#}$/ kJ mol^{-1}	$\Delta G^{\#}$/ kJ mol^{-1}
[VO(TSB-1)]·0.5H_2O	40–150	3.21	0.00	–102.00	0.33	38.1	3.47	–102.63	0.41	38.18
	150–300	9.74	1.00	–100.37	5.14	60.6	10.28	–100.18	5.68	61.12
	300–810	109.14	1.00	–92.00	104.08	160.2	113.6	–91.85	108.53	164.52
[VO(TSB-2)]·0.5H_2O	40–140	3.34	0.00	–102.00	0.24	37.65	3.97	–102.09	0.95	38.01
	140–290	7.61	1.00	–101.21	3.08	58.24	8.24	–100.92	3.71	58.71
	290–780	105.35	1.00	–92.06	100.45	154.64	107.12	–91.94	100.22	156.38
[VO(TSB-3)]·0.5H_2O	40–140	3.31	0.00	–102.04	0.13	37.43	3.14	–102.92	0.14	37.29
	140–310	6.68	1.04	–101.60	2.24	56.50	5.92	–102.04	1.48	55.97
	310–780	101.48	0.98	–92.10		150.33	99.66	–92.17	94.81	148.55
[Cu(TSB-1)]·1.5H_2O	40–150	4.86	0.00	–101.36	0.17	40.09	4.51	–101.87	1.28	40.81
	150–530	17.21	1.02	–98.16	12.81	64.74	16.92	–98.22	12.52	64.48
	530–760	137.19	1.00	–92.82	129.19	218.48	134.3	–92.90	126.30	215.67
[Cu(TSB-2)]·1.5H_2O	40–130	4.62	0.00	–101.58	1.57	38.85	4.09	–102.02	1.04	38.48
	130–510	14.15	1.00	–98.86	9.86	60.78	15.43	–98.45	11.15	61.85
	510–740	136.23	1.00	–92.84	128.59	213.92	138.81	–93.96	127.71	253.15
[Cu(TSB-3)]·1.5H_2O	40–140	4.96	0.00	–101.27	1.95	38.61	5.17	–101.13	2.16	38.77
	140–490	13.32	0.96	–98.96	9.06	59.73	14.02	–98.78	9.76	60.34
	490–710	129.57	1.01	–92.56	122.12	210.05	134.30	–93.97	123.54	245.14

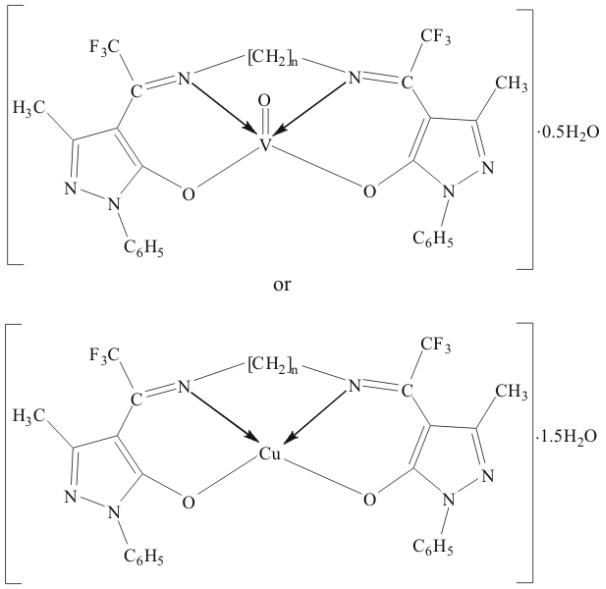

Fig. 6 The tentative structure of the complexes

the valence shell of the central ion. Both vanadium and copper ions in the investigated complexes have multiple bonding (four or five bonds) in their valence shells. But due to small ionic size of vanadium which in turn alters the bond angles from those of ideal square-pyramidal, giving lower stability [39]. Based on the above results, the tentative structure of the complexes can be formulated as shown in Fig. 6.

Conclusions

The kinetic parameters in non-isothermal conditions are investigated. The complexes decomposed in mainly three-step processes and it was observed that all of these decomposition steps are of first order reactions (except dehydration steps). The negative $\Delta S^{\#}$ values for all decomposition steps in the complexes indicate that the complexes are more ordered.

References

1 A. Garoufis, S. Kasselouri, C. A. Mitsopoulou, J. Sletten, C. Papadimitriou and N. Hadjiliadis, Polyhedron, 18 (1999) 39.
2 G. A. Kolawole and K. S. Patel, J. Chem. Soc., Dalton, (1981) 1241.
3 G. V. Panova, V. M. Potapov, I. M. Turovets and E. G. Golub, Zh. Obshch. Khim., 53 (1983) 1612; English translation: J. Gen. Chem. USSR, 53 (1983) 1452.
4 S. K. Shaikhutdinov, A. N. Shupik and E. M. Trukhan, J. Chem. Soc., Faraday Trans., 89 (1993) 3959.
5 L. C. Nathan, J. E. Koehne, J. M. Gilmore, K. A. Hannibal, W. E. Dewhirst and T. D. Mai, Polyhedron, 22 (2003) 887.
6 C. L. Albano, R. Sciamanna, T. Aquino and J. J. Martinez, European Congress on Computational Methods in Applied Sciences and Engineering, ECOMAS 2000, Barcelona, 11–14 September, 2000.
7 F. Carrasco, Thermochim. Acta, 213 (1993) 115.
8 A. A. Soliman, J. Therm. Anal. Cal., 63 (2001) 221.
9 A. F. Petrovic, D. M. Petrovic, V. M. Leovac and M. Budimir, J. Therm. Anal. Cal., 58 (1999) 589.
10 G. G. Mohamed, F. A. Nour-El Dien and E. A. El-Gamel, J. Therm. Anal. Cal., 67 (2002) 135.
11 M. Sekerci and F. Yakuphanoglu, J. Therm. Anal. Cal., 75 (2004) 189.
12 G.-C. Xu, L. Zhang, L. Liu, G.-F. Liu and D.-Z. Jia, Thermochim. Acta, 429 (2005) 31.
13 C. K. Modi and B. T. Thaker, Indian J. Chem., 41A (2002) 2544.
14 I. A. Patel, P. Patel, S. Goldsmith and B. T. Thaker, Indian J. Chem., 42(A) (2003) 2487.
15 K. R. Surati and B. T. Thaker, J. Coord. Chem., 59 (2006) 1191.
16 B. T. Thaker, K. R. Surati, S. Oswal, R. N. Jadeja and V. K. Gupta, Struct. Chem., 18 (2007) 295.
17 D. D. Perrin, W. L. F. Armarego and D. R. Perrin, Purification of Laboratory Chemicals, 2nd Edn. Pergamon Press, New York 1981.
18 E. C. Okafor, Talanta, 29 (1982) 275.
19 H. A. Flaschka, EDTA Titrations, Pergamon Press, New York 1956, p. 78.
20 I. A. Patel, B. T. Thaker and P. B. Thaker, Indian J. Chem., 37(A) (1998) 429.
21 I. A. Patel and B. T. Thaker, Indian J. Chem., 38A (1999) 427.
22 Z. T. Maqsood, K. M. Khan, U. Ashiq, R. A. Jamal, Z. H. Chohan, M. Mahroof-Tahir and C. T. Supuran, J. Enz. Inhb. Med. Chem., 21 (2006) 37.
23 M. Mohapatta, V. Chakravortty and K. C. Das, Polyhedron, 8 (1989) 1509.
24 J. D. Joshi, S. D. Patel and G. P. Patel, J. Macromol. Sci. Part A: Pure Appl. Chem., 44 (2007) 65.
25 N. Raman, Y. Pitchaikaniraja and A. Kulandaisamy, Proc. Indian Acad. Sci., 113 (2001) 183.
26 J. Selbin, Coord. Chem. Rev., 1 (1965) 293.
27 V. Ravinder, S. J. Swamy, S. Srihari and P. Lingaiah, Polyhedron, 4 (1985) 1511.
28 S. S. Dodward, R. S. Dhamnaskar and P. S. Prabhu, Polyhedron, 8 (1989) 1748.
29 K. G. Dutton, D. Fallon and K. S. Murray, Inorg. Chem., 27 (1988) 34.
30 I. S. Ahuja and S. Tripathi, Indian J. Chem., 30A (1991) 1060.
31 R. L. Dutta and A. Syamal, Elements of Magneto Chemistry, 2nd Edn. East–West Press, New Delhi 1993.
32 S. Sujatha, T. M. Rajendiran, R. Kannappan, R. Venkatesan and P. S. Rao, Proc. Indian Acad. Sci., 112 (2000) 559.
33 E. S. Freeman and B. Carroll, J. Phys. Chem., 62 (1958) 394.

34 H. H. Horowitz and G. Metzger, Anal. Chem., 25 (1963) 1464.
35 P. B. Pansuriya and M. N. Patel, Appl. Organomet. Chem., 21 (2007) 739.
36 C. K. Modi, S. H. Patel and M. N. Patel, J. Therm. Anal. Cal., 87 (2007) 441.
37 M. Sekerci and F. Yakuphanoglu, J. Therm. Anal. Cal., 75 (2004) 189.
38 H. M. Parekh, P. K. Panchal and M. N. Patel, J. Therm. Anal. Cal., 86 (2006) 803.
39 G. G. Mohamed and Z. H. Abd El-Wahab, J. Therm. Anal. Cal., 73 (2003) 347.

Received: November 25, 2007
Accepted: June 19, 2008
OnlineFirst: Septemer 20, 2008

DOI: 10.1007/s10973-007-8645-z